Monitoring CO_2 Injection at Weyburn Reservoir Using 3-D/3-C Seismic Datasets*

Le Gao[1] and Igor Morozov[1]

Search and Discovery Article #20290 (2015)
Posted January 19, 2015

*Adapted from extended abstract prepared in conjunction with presentation at CSPG/CSEG/CWLS GeoConvention 2013, (Integration: Geoscience engineering Partnership) Calgary TELUS Convention Centre & ERCB Core Research Centre, Calgary, AB, Canada, 6-12 May 2013, Datapages/CSPG © 2015

[1]University of Saskatchewan, Saskatoon, Saskatchewan, Canada (le.gao@usask.ca)

Abstract

In order to monitor and verify the distribution of CO_2 during its geologic storage and enhanced oil recovery in Weyburn oil field in Saskatchewan, Canada, we applied the time-lapse AVO (amplitude variation with offset) method to time-lapse 3-D/3-C seismic datasets. Standard AVO attributes, such as intercept, gradient, S-wave reflectivity, together with additional empirical attributes are compared using three vintages of the data from 1999 to 2002. The results indicate that pressure-saturation effects related to the presence of CO_2 can be identified between horizontal injection wells.

Introduction

The Weyburn-Midale field in southeast Saskatchewan is the site of one of the earliest, largest and most advanced CCS (Carbon Capture and Storage) projects. The field has been undergoing CO_2 injection since October 2000. In order to monitor CO_2 injection, storage, and oil recovery, 3-D seismic datasets were acquired annually, starting from a baseline survey in December 1999 (White, 2009). In this study, we use three-component surface datasets of the baseline and two monitor surveys conducted in 2001 and 2002. The main objective of seismic monitoring is to track and quantify the distribution of CO_2 in the subsurface. The principal challenges, and the keys to successful CO_2 sequestration in this field are the ability to differentiate between the pore-pressure and CO_2 saturation effects, calibration of the different vintages of the data, and the accuracy required for monitoring a very thin reservoir. Among the various seismic techniques for measuring the CO_2 content in the subsurface, variations of time intervals between the reflectors and Amplitude Variations with Offset (AVO) appear to be most promising.

Time-Shift and AVO Results from Weyburn 3-D 3-C Datasets

In order to compare the time and amplitude variations between the monitor (2001 or 2002) and baseline datasets (1999), the amplitudes and phases of the records need to be equalized. The equalization is achieved by pre-stack calibration (Gao and Morozov, 2010) and by picking a continuous reference horizon above the reservoir and measuring the stacked reflection amplitude at it. Figure 1 shows three of such reference horizons: R1, R2 and R3. For all the AVO attributes here, R3 is used for normalization.

Before measuring the variation of AVO attributes, we examined the differences in the two-way travel times for several reference horizons. The time shifts between the monitor and baseline datasets were picked from the maxima of cross-correlations on the stacked section within narrow time windows (20 ms). To quantify the injection-related changes above the reservoir, it is most important to measure the variation in the time intervals between reflectors, which should increase with increasing pore pressure and fluid content. Figure 2 shows the change in the reflection-time interval between the caprock and Bakken (~150 ms below reservoir). The two-way travel time variation is ~1 ms, and positive time anomalies are correlated with the injection wells, particularly for 2002 monitor in the SE part of the survey area (Figure 2). Taking a ~5% P-wave velocity reduction as an estimate for the effect of CO_2, this would mean that 20~30-m below the caprock might be affected by the CO_2 after two years of injection, in the areas shown by red colour in Figure 2.

The two-term AVO analysis was based on measuring the intercept (I), and gradient (G) near the reservoir, from which several secondary attributes were derived. Based on Shuey's approximation (Shuey, 1985), for compressional (P) waves, the reflection coefficient R, is related to the incidence angle (θ) as:

$$R(\theta) = I + G\sin^2\theta \qquad (1)$$

Using the measured I and G, we also derived the combinations: $(I\text{-}G)/2$ (approximation for the S-wave reflectivity) and $I+G$ (Gao and Morozov, 2010). From fluid substitution modeling for this reservoir, such combinations should be sensitive to pore-pressure and CO_2 saturation, respectively (Ma and Morozov, 2010). In addition, two additional secondary attributes with similar properties were derived empirically by projecting the (I,G) points onto the directions along and across the trend line of the empirical distribution of AVO parameters (Figure 3). Point (I_C,G_C) in Figure 4 is the center of the distribution of all (I,G) values picked for Marly horizon and (I_0,G_0) is the projection of (I,G) onto the trend line. Assuming that the trend is due to the variations of pore pressure within the reservoir, positive values (red colors in the plots below) of $\delta P1$ and $\delta P2$ correspond to the directions of increasing pressure and decreasing CO_2 saturation, respectively (Ma and Morozov, 2010).

Figure 4 and Figure 5 show the AVO intercepts and gradients respectively at the Marly. Figure 6 shows that the S-wave reflectivity at the Marly reflection, which appears to be more sensitive to pore-pressure changes. Figure 7 shows the AVO attribute $I+G$, which is more sensitive to CO_2 saturation variation. Maps of attributes $\delta P1$ and differential attribute $\delta P2$ for Marly reflector are shown in Figure 8 and Figure 9.

Conclusions

Variations of time intervals between reflections within the Weyburn reservoir during CO_2 injection show effects of injection fluids amounting in ~30-m below caprock. The travel time delays below the reservoir indicate the increasing travel time when reflections passing through the reservoir during CO_2 injection. AVO modeling for this reservoir suggests that positive correlations between the intercept and gradient (such as $I+G$) should be most sensitive to saturation whereas auto-correlated anomalies ($I\text{-}G$) are indicators of pore pressure. From these time-lapse attributes, we recognized the pore-pressure and CO_2 saturation variations during the first two years of monitoring (2001 and 2002). The results show good correlation with several injection wells and indicate that the AVO technology can help estimating the in-situ reservoir pressure and fluid saturation variations from time-lapse seismic data.

Acknowledgements

The work is funded by Phase II of IEA GHG Weyburn CO_2 Storage Monitoring Project.

References Cited

Gao, L., and I.B. Morozov, 2010 AVO analysis of 3-D/3-C datasets: 2010 CSPG/CSEG/CWLS Convention.

Ma, J., and I.B. Morozov, 2010, AVO modeling of pressure-saturation effects in Weyburn CO_2 sequestration: The Leading Edge, v. 29, p. 178–183.

Shuey, R.T., 1985, A simplification of the Zoeppritz equations: Geophysics, v. 50, p. 609-614.

White, D., 2009, Monitoring CO_2 storage during EOR at the Weyburn-Midale field: The Leading Edge, v. 28, p. 838-842.

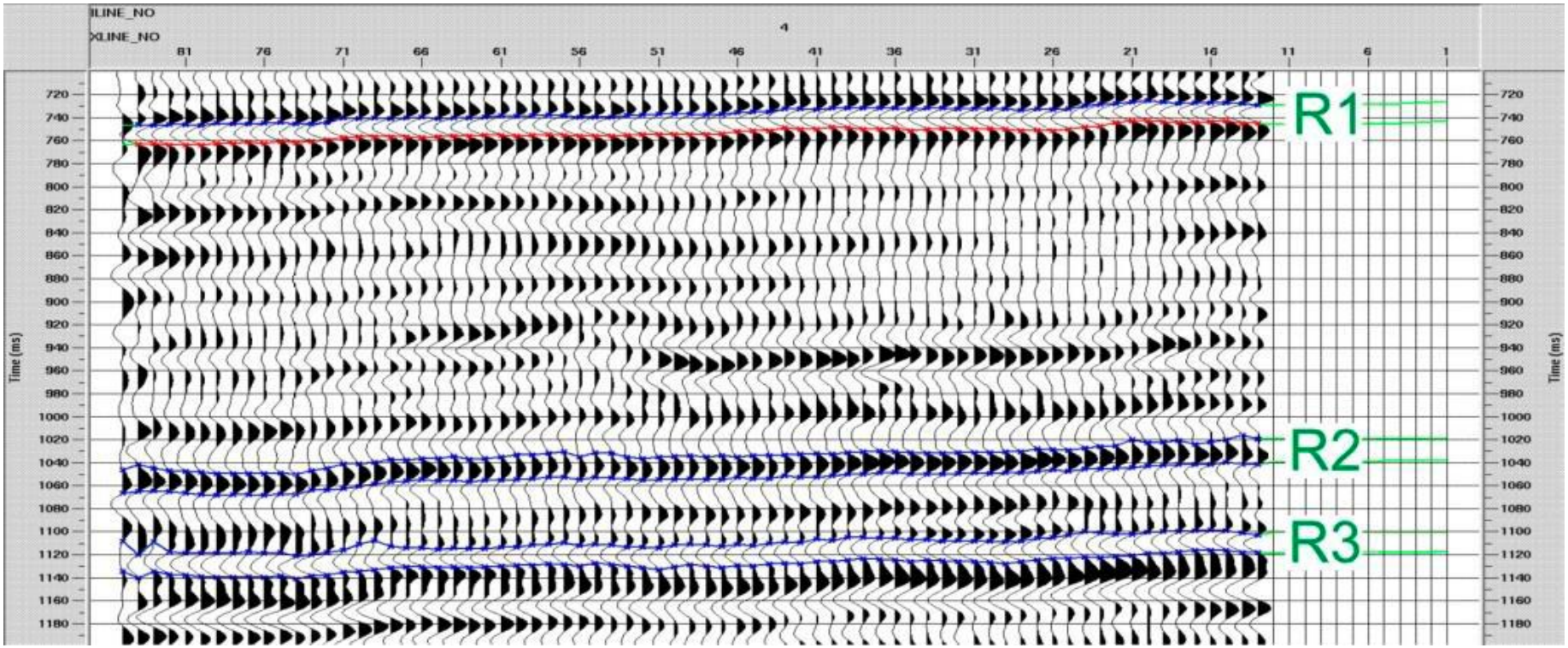

Figure 1. Reference horizons (green labels) used for calibration of reflection and AVA responses.

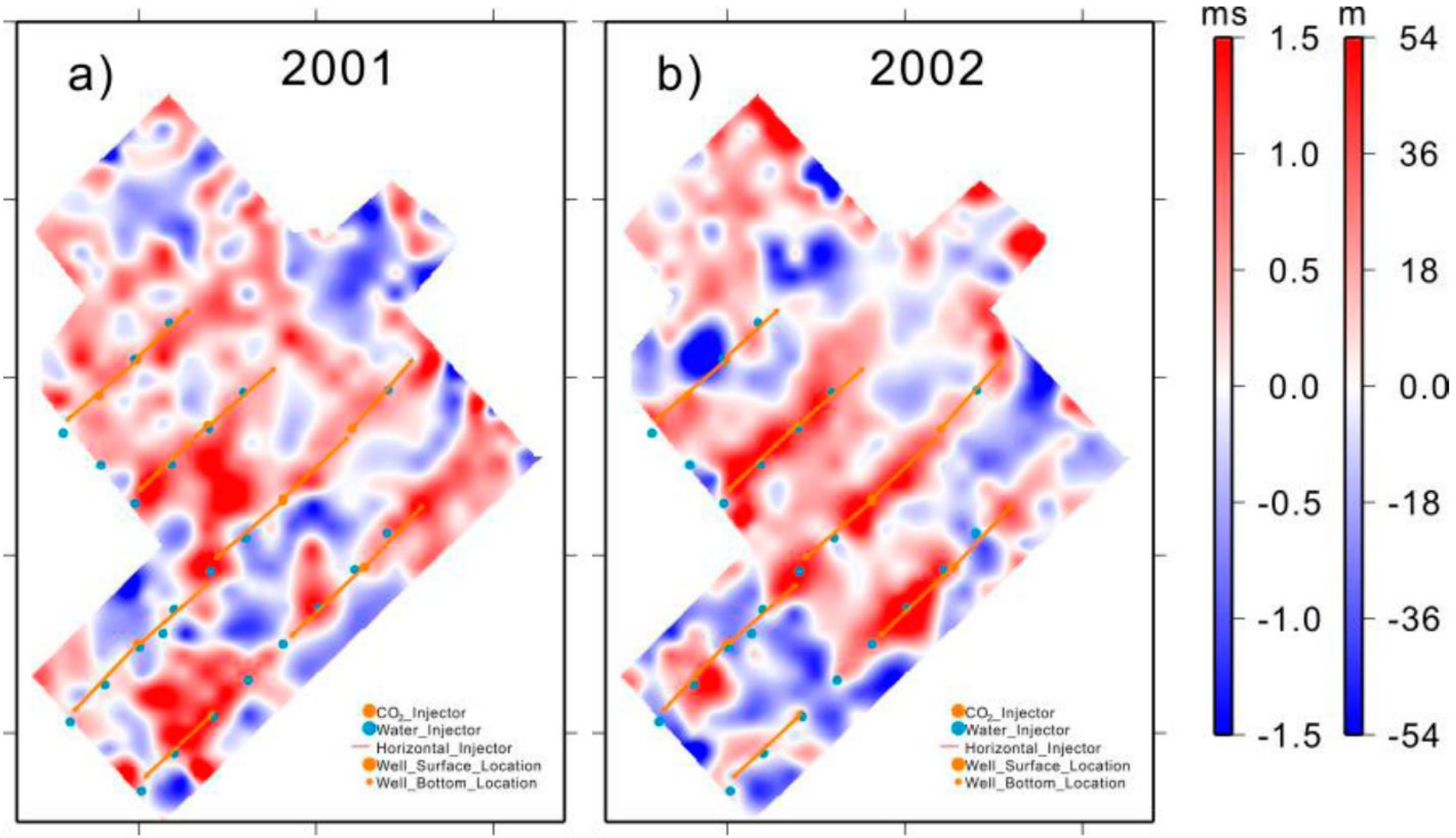

Figure 2. Variations of time differences and thickness between the caprock reflector and Bakken (~200ms below caprock). a) 2001 relative to 1999; b) 2002 relative to 1999. The colour bar on the right gives the estimated thickness of the fluid-affected zone below the caprock.

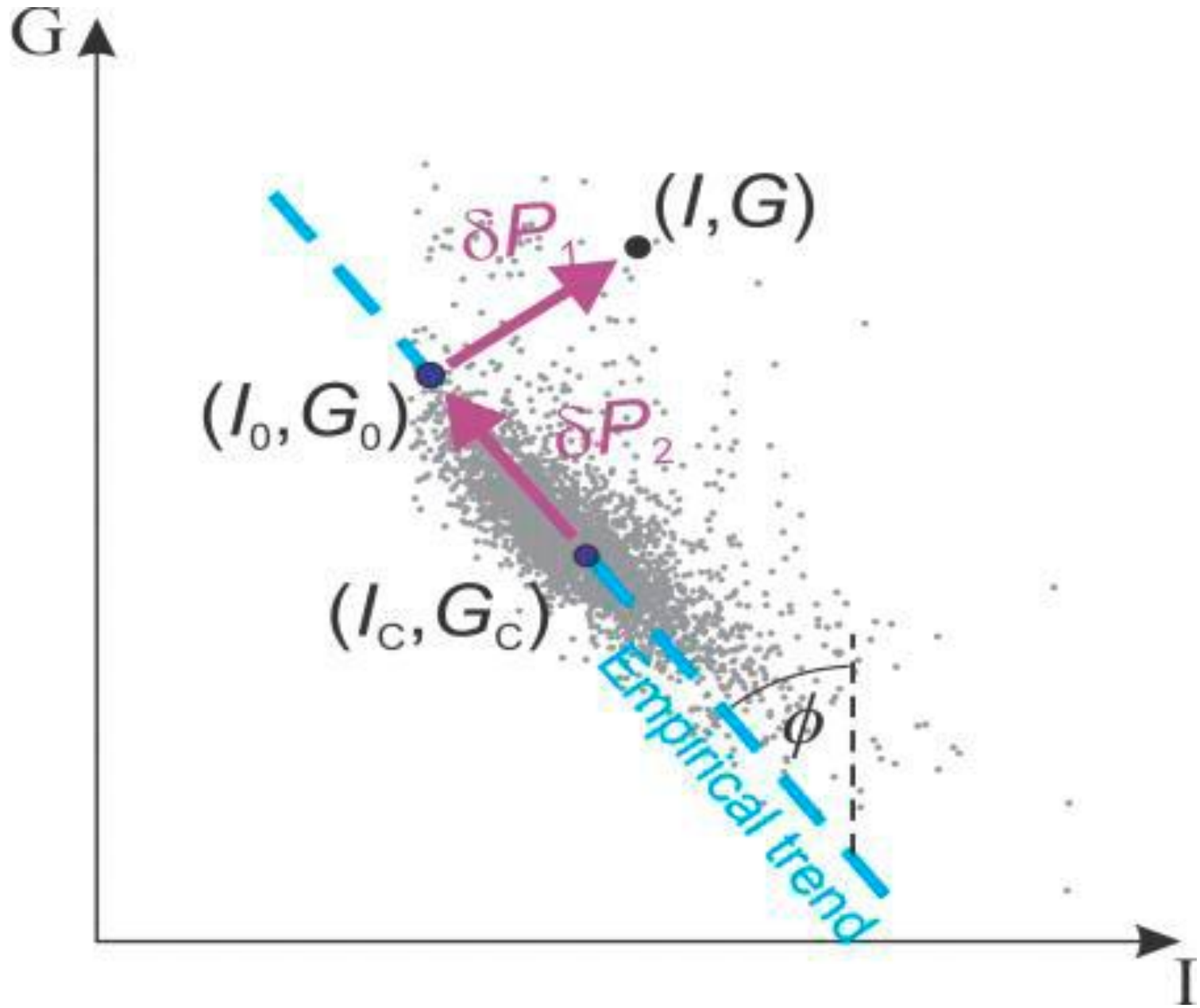

Figure 3. Empirical proxy attributes emphasizing the deviations of AVO parameters along (*δP1*) and across the trend line (*δP2*). Grey dots are the measured AVO points.

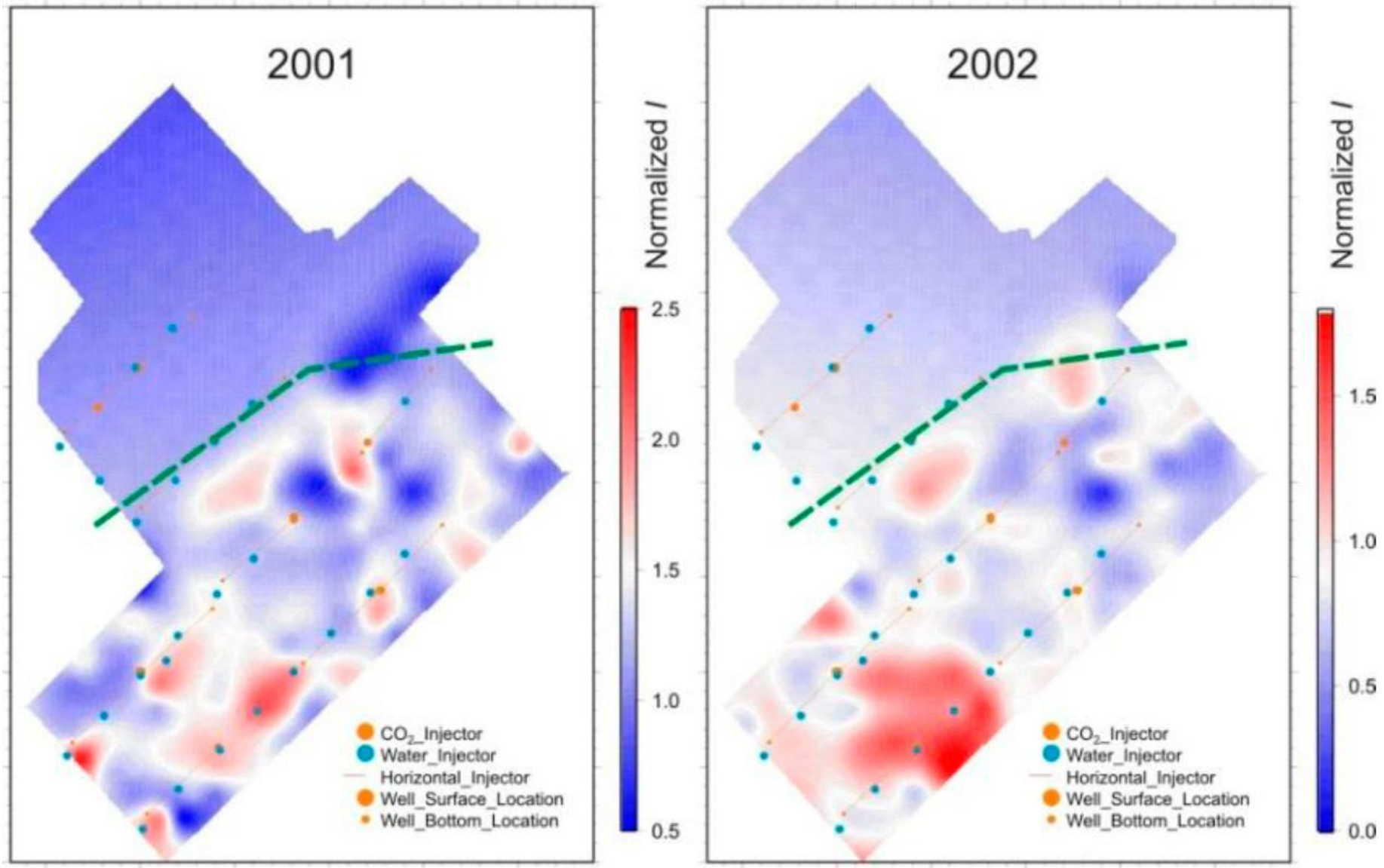

Figure 4. Variations of the calibrated AVO intercepts at Marly reflection for two monitor datasets (labeled). Green dashed line indicates the approximate extent of picked Marly reflection.

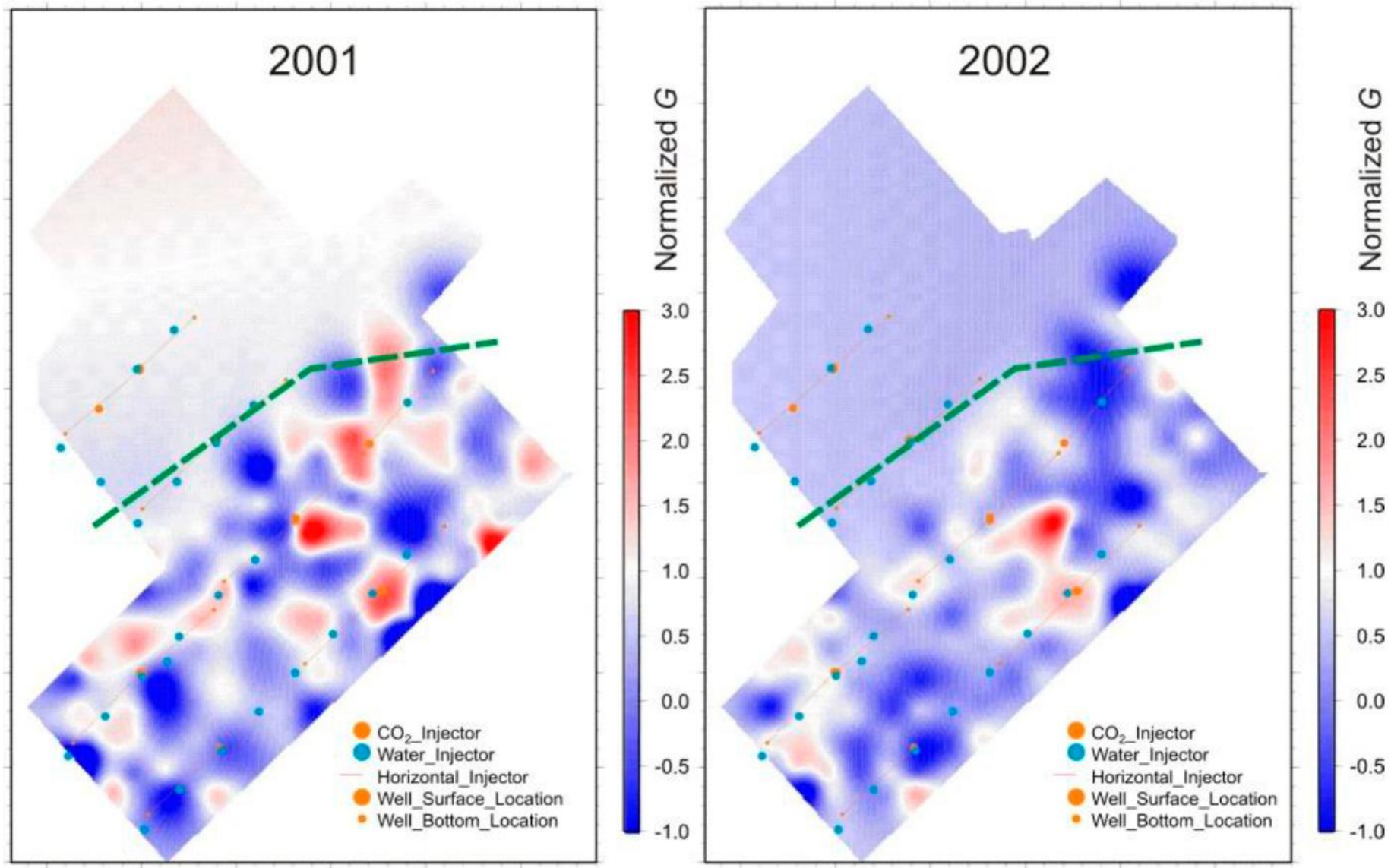

Figure 5. Variations of the calibrated AVO gradients at Marly reflection for two monitor datasets (labeled).

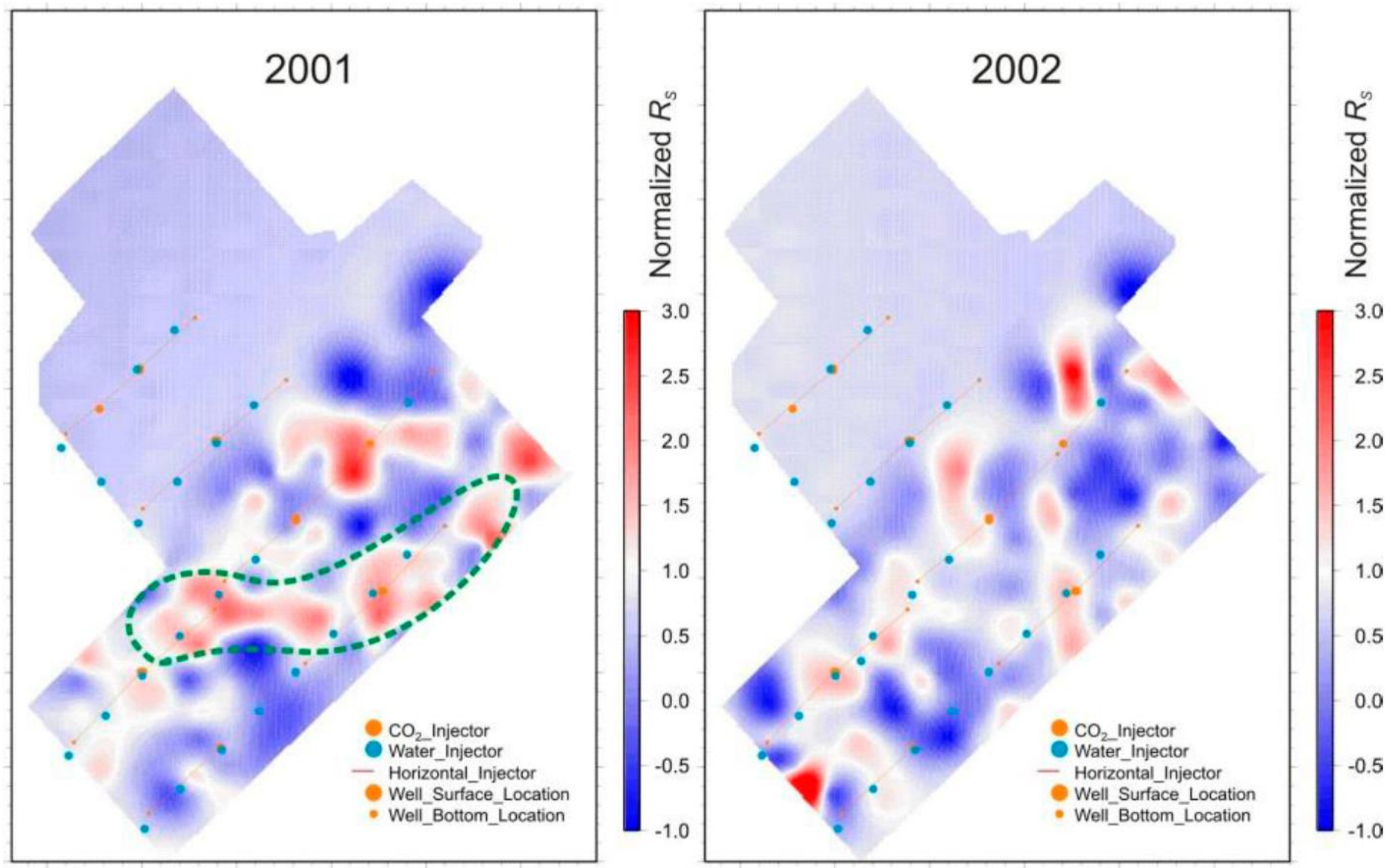

Figure 6. Variations of the calibrated S-wave reflectivity (*I*–*G*) at Marly for two monitor datasets (labeled). Dashed green line indicates the interpreted area of increased pore pressure.

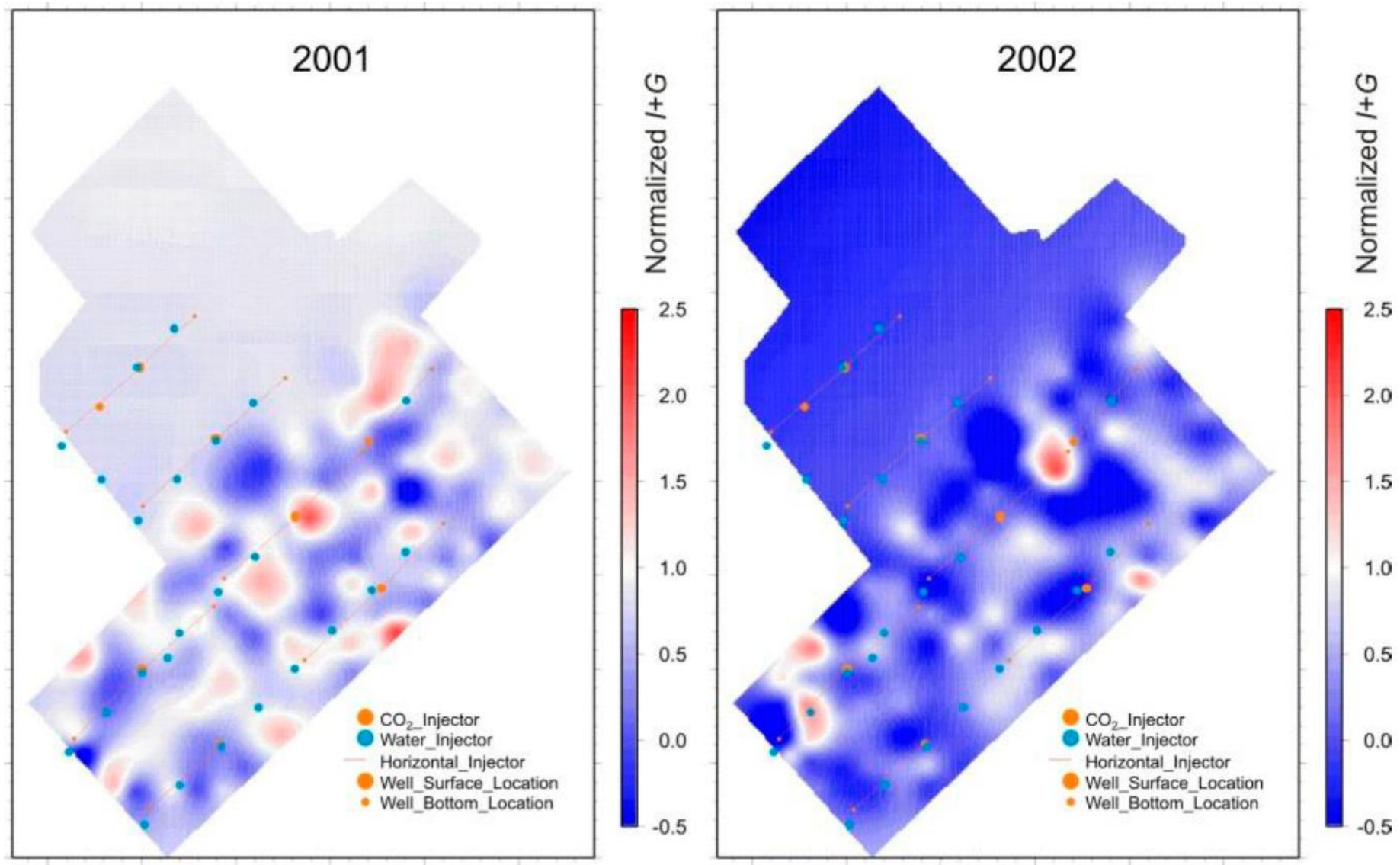

Figure 7. Combination of AVA attributes *I*+*G* for Marly reflection.

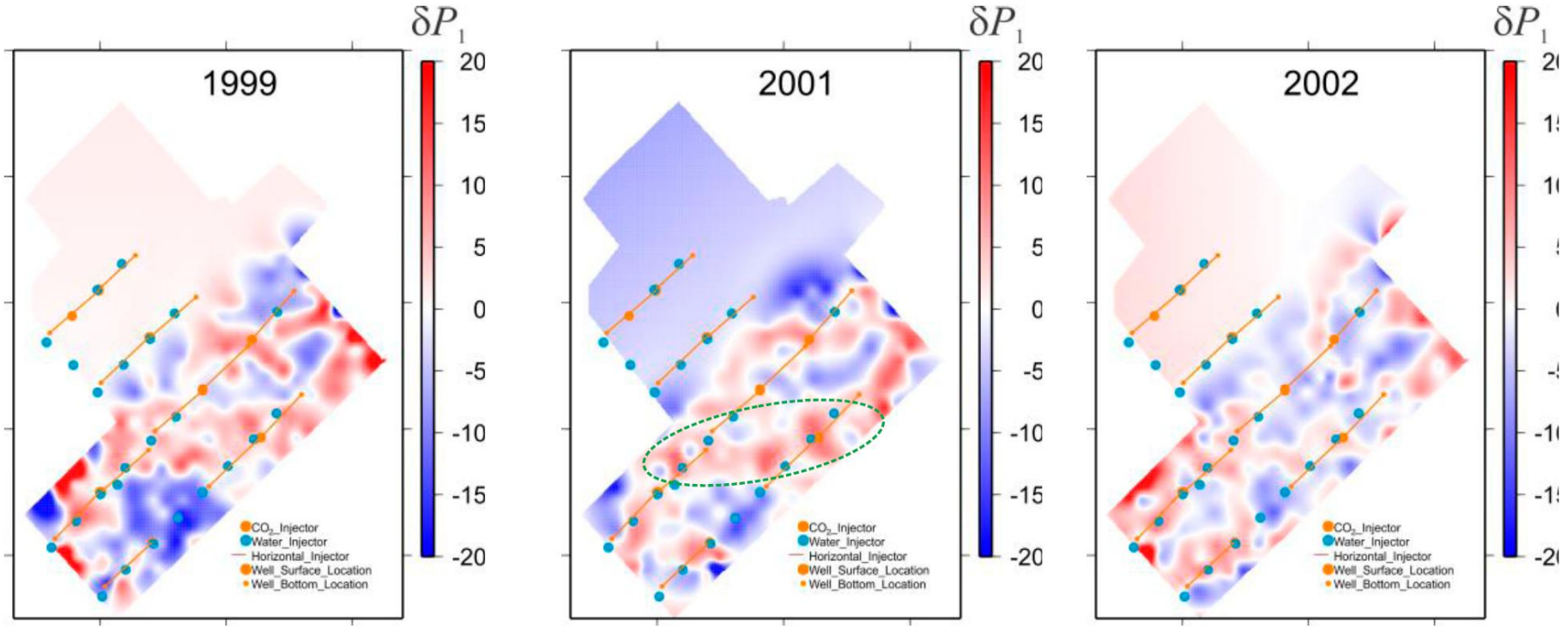

Figure 8. Attribute *δP1* for Marly reflection for each of the three vintages of the dataset. Dashed green ellipse indicates the area of increased pore pressure.

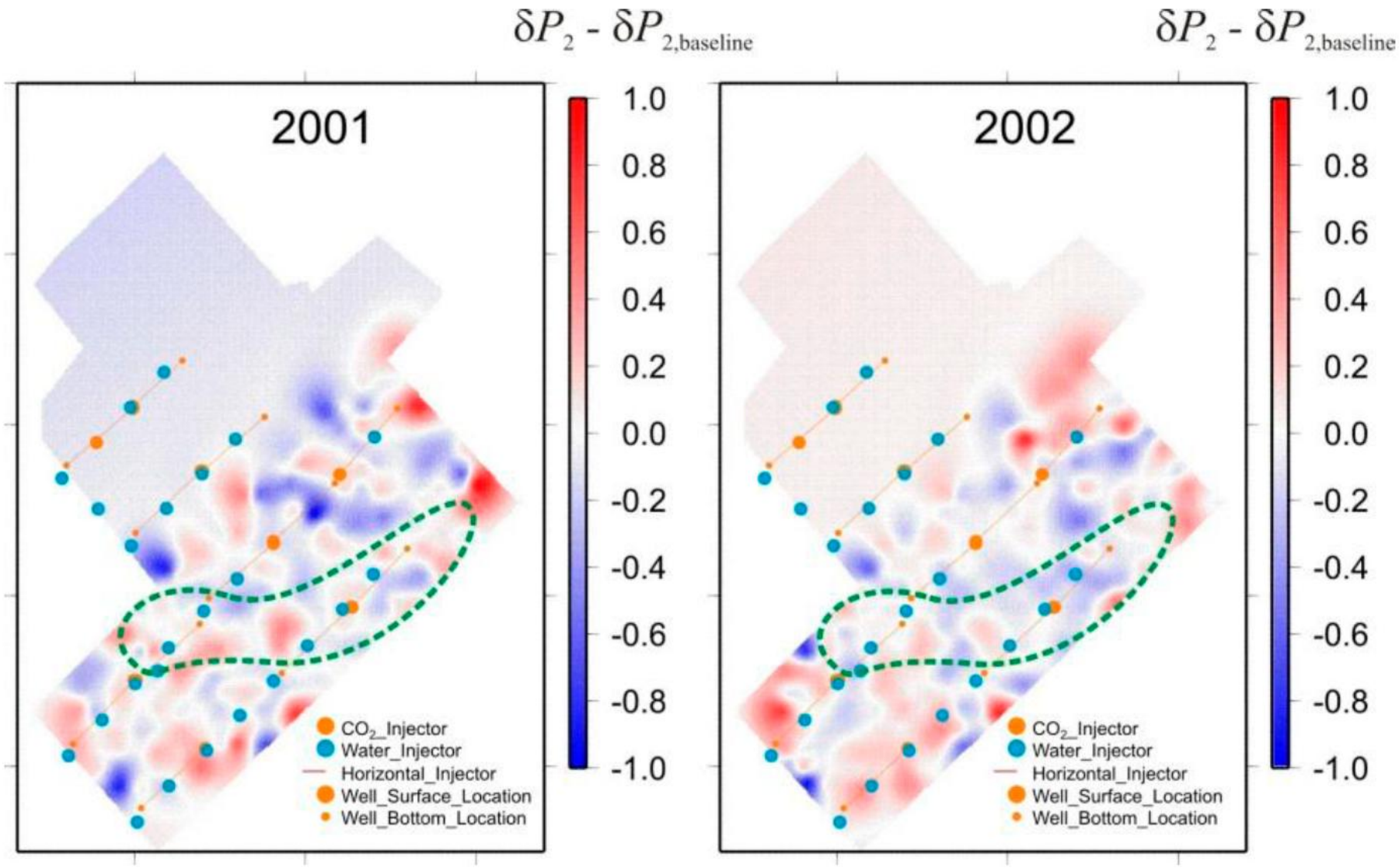

Figure 9. Differential attribute *δP2* for Marly reflection. Dashed green lines indicate the interpreted area of increased CO_2 saturation.